# On the ground–state energy of finite Fermi systems

Jérôme Roccia and Patricio Leboeuf
*Laboratoire de Physique Théorique et Modèles Statistiques,*
*CNRS, Bât. 100,*
*Université de Paris-Sud, 91405 Orsay Cedex, France*

(Dated: February 9, 2008)

We study the ground–state shell correction energy of a fermionic gas in a mean–field approximation. Considering the particular case of 3D harmonic trapping potentials, we show the rich variety of different behaviors (erratic, regular, supershells) that appear when the number–theoretic properties of the frequency ratios are varied. For self–bound systems, where the shape of the trapping potential is determined by energy minimization, we obtain accurate analytic formulas for the deformation and the shell correction energy as a function of the particle number $N$. Special attention is devoted to the average of the shell correction energy. We explain why in self–bound systems it is a decreasing (and negative) function of $N$.

PACS numbers: 21.10.Dr, 03.65.Sq, 21.60.-n



## I. INTRODUCTION

When estimating the ground–state energy of interacting Fermi gases, one can schematically rely on two different approaches. For few–particle systems (say, less than 10-20), direct *ab initio* calculations are available at present [1]. For larger systems, and in particular for global mass calculations in atomic nuclei, approximate schemes based either on mean–field calculations [2] or shell models [2, 3] are inevitable. In mean field theories, in which we focus here, the energy or mass of the system is naturally decomposed into a smooth part and a fluctuating part. Methods like Thomas-Fermi (TF) or Wigner-Kirkwood theories provide an approximation to the smooth part [2, 4], whereas the oscillatory shell structure may be described by semiclassical methods [4]. In practice, these two contributions may be well separated in a grand canonical scheme, where the energy is considered as a function of the chemical potential $\mu$: the TF contribution describes the smooth dependence on chemical potential, whereas the oscillatory component has *zero average* (with respect to $\mu$) and describes deviations with respect to the mean behavior.

In isolated systems with a well defined number of particles $N$, things are different. When the dependence of the ground–state energy $E(N)$ is considered as a function of $N$, one can show [5] that its fluctuating part, $\widetilde{E}(N)$, in contrast to usual expectations, has a non–zero average (as a function of $N$). It follows that the fluctuating part contributes to the smooth part $\bar{E}(N)$ of the energy, and the frontier between smooth and fluctuating components is blurred. This is a generic effect, although its importance depends on the symmetries (and intrinsic dynamics) of the mean field potential. A description of this effect was recently developed [5] for a confining potential which keeps its shape fixed (up to a possible scaling factor) when the number of particles varies (cf Eq. (6) below).

Although the latter situation may be relevant in many experimental set–ups, like cold dilute Fermi gases in magnetic atom traps [6], where the external HO potential dominates over the mean–field interaction energy [7], another relevant case is that of self–bound systems, like the atomic nucleus. In these systems, an effect that was not included in the previous description appears: the shape of the average self–bound confining potential depends on the number of particles. As is well known, at a given $N$ the shape is determined by minimizing the energy of the system. The minimization of the smooth part of the energy leads generically to an isotropic shape. We denote this contribution $\bar{E}_{sph}(N)$. For that shape, and for particular values of $N$ (magic numbers) the contribution of the fluctuating part $\widetilde{E}_{sph}(N)$ is large and negative, thus reducing the total energy with respect to $\bar{E}_{sph}(N)$. Away from magic numbers, the amplitude of $\widetilde{E}_{sph}(N)$ rapidly decreases, and may eventually become positive. In order to avoid this behavior, the system deforms, trying to keep the value of the oscillating part of the self–bound energy $\widetilde{E}_{SB}(N)$ negative and as large as possible. Though in most realistic situations $\widetilde{E}_{SB}(N) \ll \bar{E}(N)$, the behavior of $\widetilde{E}_{SB}(N)$ has a strong influence on the shape of the system. Schematically (see Fig.4), the behavior of $\widetilde{E}_{SB}(N)$ is therefore a fluctuating negative function of $N$, with larger amplitudes around the magic numbers.

It follows that in self–bound systems, as for Fermi gases confined by a fixed external potential, the average part of the energy fluctuations is again generically different from zero. However, the properties of the average are very different in these two cases. In particular, the average is positive for a fixed shape, while it is negative in self–bound systems. Such a bias toward negative energies of the fluctuating part in self–bound systems is clearly observed in realistic calculations [5]. In the bottom part of Fig. 5 we plot the nuclear ground–

state shell correction energy computed in Ref.[8] using a macroscopic–microscopic model, whose results are in good agreement with experimental data. We do observe a tendency toward negative values, with a non-zero slope for the average part of the fluctuations. One of our purposes here is to provide a quantitative description of this effect.

We will consider the case of non–interacting fermions in 3D whose self–bound confining potential is assumed to have a quadratic harmonic shape. The reason for such a choice is purely technical, since it allows, to some extent, for an explicit analytic description. In spite of its simplicity, we will show that it provides a correct description of what is observed in more realistic calculations.

Harmonic potentials were intensively investigated in the past, starting from the Nilsson model of the nuclear deformation [9]. This is an integrable (separable) model. It is known that the statistical properties of its single–particle spectrum do not coincide with the generic (Poisson) behavior expected in integrable systems [10]. The statistics, explored mainly in D=2, are in fact very sensitive to the number theoretic properties of the frequency ratios [10, 11]. As we will show, these number theoretic properties also strongly influence the behavior of the many body system.

Our analysis of the minimization of the energy of the Fermi gas will be based on a semiclassical theory. Though this theory is exact for the single–particle density of states, the different cases (of irrational or rational frequency ratios) should, however, be considered carefully [11]. We shall see that the amplitude and phase of shell effects are directly controlled by the number–theoretic properties of the frequencies. The output of the minimization problem thus depends on a delicate interplay between these number–theoretic properties and the number of particles in the gas.

The manuscript is organized as follows: in section II we study the main properties of $\widetilde{E}(N)$ for an harmonic potential of given frequency ratios. We will illustrate the large variety of different behaviors that could emerge (including shell and supershell structures). In section III, we deal with the case of self–bound systems, and apply our results to a schematic model of the atomic nucleus (that we compare to realistic calculations).

## I. GENERAL SETTING

For a given potential the single–particle level density is decomposed into a smooth part $\bar{\rho}$ coming from the TF theory plus an oscillatory contribution $\widetilde{\rho}$:

$$\rho(\epsilon) = \bar{\rho}(\epsilon) + \widetilde{\rho}(\epsilon) \ . \tag{1}$$

Here, $\epsilon$ is the single–particle energy. Below, we will show in more detail how to describe these two components. The spin degeneracy is included in the level density. Equation (1) induces a corresponding decomposition of the integrated level density (that counts the number of single–particle states up to an energy $\mu$):

$$\mathcal{N}(\mu) = \bar{\mathcal{N}}(\mu) + \widetilde{\mathcal{N}}(\mu) = \int_0^\mu \bar{\rho}(\epsilon)\, d\epsilon \ + \int_0^\mu \widetilde{\rho}(\epsilon)\, d\epsilon \ . \tag{2}$$

In order to study a system with a finite number of particles, we use canonical expressions for thermodynamic quantities. For a system of $N$ non–interacting fermions, we define its ground state energy $E(N)$, the shell correction energy $\widetilde{E}(N)$ and the smooth TF component $\bar{E}(N)$ as [2, 4]:

$$\widetilde{E}(N) = E(N) - \bar{E}(N) = \int_0^{\mu_N} \epsilon\rho(\epsilon)d\epsilon - \int_0^{\bar{\mu}_N} \epsilon\bar{\rho}(\epsilon)d\epsilon. \tag{3}$$

The chemical potential $\mu_N$ and its smooth part $\bar{\mu}_N$ fix the number of particles. They are defined by inversion of the exact and average integrated level densities, $\mathcal{N}(\mu_N) = N$ and

$$\bar{\mathcal{N}}(\bar{\mu}_N) = N \ , \tag{4}$$

respectively. Unfortunately, Eq.(3) is difficult to exploit analytically because the discretization of $\mu_N$ is difficult to impose. From Eq.(3) it can be shown that, neglecting terms of second order in the parameter $\mu - \bar{\mu}$, $\widetilde{E}$ may be approximated by [12, 13]:

$$\widetilde{E}(N) \approx -\int_0^{\bar{\mu}_N} \widetilde{\mathcal{N}}(\epsilon)d\epsilon \ . \tag{5}$$

This, together with the definition of $\bar{E}(N)$, are the basic equations upon which our analysis of ground state energies of Fermi gases will be based on.

If, in Eq. (5), $\bar{\mu}_N$ is considered as a continuous variable, it can easily be shown that it gives a wrong result for the average of the fluctuating function $\widetilde{E}(N)$. Indeed in a system with a fixed number of particles, the chemical potential takes discrete values as $N$ varies. The fluctuating part of the ground state energy is sampled at particular values of the chemical potential, implying a modification of its average value. Recently, an explicit description for this effect was given. It was found that the contribution of the fluctuating part to the average of the energy is given by [5]

$$\langle\widetilde{E}(N)\rangle_N \approx \langle\widetilde{\mathcal{N}}^2(\bar{\mu}_N)\rangle_{\bar{\mu}_N} / \bar{\rho}(\bar{\mu}_N) \ , \tag{6}$$

where we use brackets to denote an average over an appropriate chemical potential window and to distinguish this contribution with respect to the TF smooth term.

## II. EXTERNAL POTENTIALS

### A. Triaxial case with irrational frequencies

We consider a particle in a 3D harmonic potential. The Hamiltonian is given by:

$$H = \frac{1}{2}(p_x^2 + p_y^2 + p_z^2) + \frac{1}{2}(Q_1^2 x^2 + Q_2^2 y^2 + Q_3^2 z^2) \ , \quad (7)$$

where all quantities are dimensionless (units $\hbar = m = 1$). $Q_1$, $Q_2$ and $Q_3$ are the frequencies of the harmonic oscillator (HO). In this subsection we considered them as incommensurable real numbers with pairwise irrational ratios. Using Eq.(2) and the expression of the TF level density $\bar{\rho}$ given in Table I, we calculate from Eq.(4) the smooth chemical potential to leading order in $N$:

$$\bar{\mu}_N = (3Q_1Q_2Q_3N)^{1/3} \ . \quad (8)$$

For irrational frequency ratios, the only periodic orbits of the system are the one–dimensional oscillations along the three principal axis $x$, $y$ and $z$. These orbits are isolated, and are the backbone for the description of the fluctuating part of the different quantities. In particular, the single particle level density $\widetilde{\rho}(\epsilon)$ was computed in [11] (using semiclassical methods based on the trace formula, which coincide with exact results obtained from the inverse Laplace transform of the exact partition function). From Eqs.(2) and (5), and the previous expression (8) of $\bar{\mu}_N$, we compute analytically the expressions for $\widetilde{\mathcal{N}}(\mu)$ and $\widetilde{E}(N)$. These, together with that of $\widetilde{\rho}$ (see Ref.[11]), are reported in Table II (first column, case A).

From periodic orbit theory (POT), it is known that the main features of the shell correction energy can be recovered by taking into account only the first (shortest) orbits [13], which correspond to the first terms in each of the three sums (lowest $k$ values) of $\widetilde{E}(N)$. As the number of particles $N$ is varied, the interferences between these terms produce an oscillatory pattern. For potentials in which the single–particle spectrum has a simple structure, like the isotropic HO discussed in the next subsection, the oscillatory pattern of the energy as a function of $N$ will be quite regular. One speaks in that case of shell effects and magic numbers (which correspond to the minima of the regular oscillation). In the present case of irrational frequency ratios, the structure of the single–particle spectrum is highly non–trivial, and leads to a complicated pattern of oscillations of the energy as a function of $N$. This is illustrated for a particular case in Fig. 1. The full line is obtained from the corresponding equation of Table II, using only the first term in each sum ($k = 1$). Although details are missing, note the good overall agreement obtained with just three orbits. Note the absence of regularity of the pattern.

As the classical orbits for irrational frequencies do not form families but are instead isolated, the amplitude of the fluctuations is small (compared to the results of, e.g., the isotropic case of the next subsection, see Fig. 2). The purely quantum mechanical counterpart of this statement is that due to the absence of symmetries in the system, no systematic degeneracies occur in the single–particle spectrum, fluctuations are small, and accordingly the energy does not deviate significantly from its average part. Moreover, the typical value of $\widetilde{\mathcal{N}}$ is also small, and we find a correction to the mean value coming from the oscillatory part, calculated from Eq.(6), that vanishes as $N^{-2/3}$ (cf [5] for further details of the method).

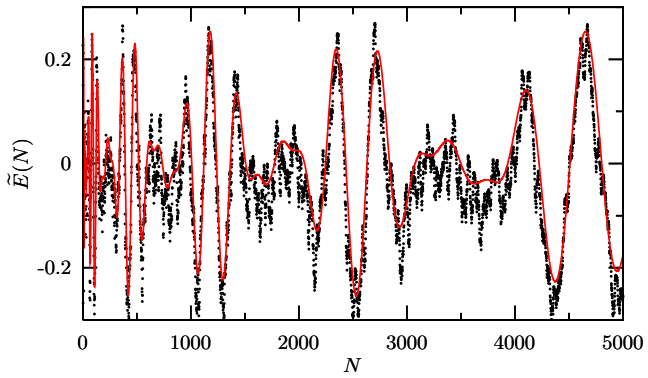


FIG. 1: (Color online) Ground state shell correction energy as a function of $N$ for $Q_1 = \sqrt{2}$, $Q_2 = \sqrt{3}$ and $Q_3 = \sqrt{5}$. Quantum computation in dots, theoretical prediction (see Table II) using the first term in each sum in full line.

### B. Isotropic case

Let's consider now the case $Q_1 = Q_2 = Q_3 = 1$. The system possesses the U(3) symmetry. Within POT, a perturbative approach of the irrational case allows to compute the level density [11], to obtain the well known result given in the top row of the second column of Table II. To compute $\widetilde{\mathcal{N}}(\mu)$ and $\widetilde{E}(N)$, we have followed the method explained above (see the results in the second column of Table II). The high degree of symmetry of the system leads in this case to a single characteristic period for the periodic orbits, implying a much more regular pattern of the shell oscillations (compare the upper part of Fig. 2 with Fig. 1). With respect to the triaxial irrational case, the amplitude of the fluctuations is much larger (this is related to the high degeneracy of the energy levels or, semiclassically, to the fact that the periodic orbits form families). The approximate frequency of the shell fluctuations is given by the phase of the cosine function of the first $k = 1$ term of the sum in $\widetilde{E}(N)$. Thus magic numbers, given by the values of $N$ that minimize $\widetilde{E}(N)$, are well approximated by

$$N_{MAGIC} = \frac{i^3}{3}, \quad \text{where } i \in \mathbb{N}^* \ , \quad (9)$$

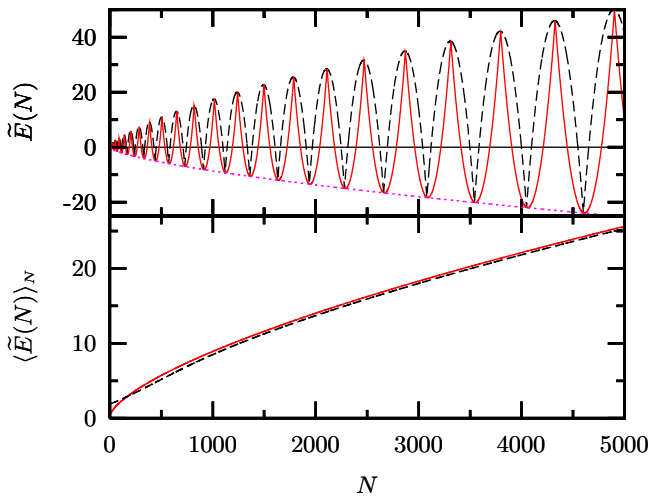


FIG. 2: (Color online) Upper panel: Ground state shell correction energy as a function of $N$ for the isotropic HO. Quantum computation in dashed line, semiclassical theoretical prediction in full line. The dotted line correspond to the analytical expression of the minima of $\widetilde{E}$ (see last row of Table II). Lower panel: Numerical average of the exact fluctuating function of the upper panel (dashed line), compared to the theoretical prediction, Eq.(6) (full line) (from Ref.[5]).

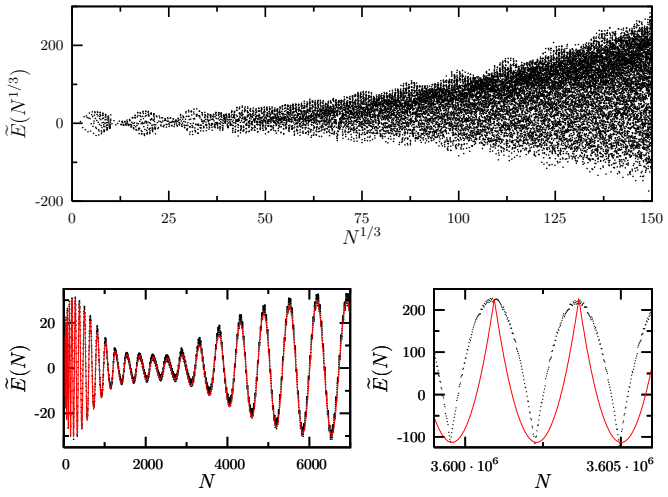


FIG. 3: (Color online) Upper panel: Ground state shell correction energy as the function of $N^{1/3}$ for $Q_1 = 17$, $Q_2 = 18$ and $Q_3 = 19$. In dots, numerical computation. We observe triaxial to isotropic transition for $\mathcal{R}_T \backsim 1$, which corresponds to $N_c = 131060$ (or $N_c^{1/3} \backsim 51$).
Lower left panel: Magnification of the upper panel for low values of $N$ ($\mathcal{R}_T > 7$). In dots, numerical computation. The full line corresponds to the analytical expression of $\widetilde{E}_T$ with the first term in each sum. The triaxial component of $\widetilde{E}$ dominates, and shows super shell effects due to interferences of the shortest orbits.
Lower right panel: Magnification of the upper panel for $N^{1/3} \backsim 150$ ($\mathcal{R}_T \backsim 0.11$). Dots, numerical computation. The full line corresponds to the analytical expression of $\widetilde{E}_I$. The isotropic component of $\widetilde{E}$ dominates. The behavior is similar to the isotropic case of Fig. 2.

which corresponds to integer values of the chemical potential $\bar{\mu}_N$.

Classically, all the orbits are closed (periodic), and have the same period. This high degeneracy of the periodic orbits is reflected in the prefactor $N^{2/3}$ in front of $\widetilde{E}(N)$ (cf Table II), as compared to the case of irrational ratios. Because there is only one characteristic frequency associated to the periodic orbits, no beating effects are observed, and the fluctuations are very regular (forming "shells"). In particular, no supershell structure is present, like the characteristic beating pattern observed in a spherical cavity with hard walls, produced by the interference between the triangular and the square orbits, see Refs.[4, 14].

In Fig. 2, we clearly see that the average of $\widetilde{E}(N)$ is non zero and positive, and increases as $N$ increases. Using in Eq.(6) the corresponding expression for $\widetilde{\mathcal{N}}(\bar{\mu}_N)$, we get an analytical expression for $\langle\widetilde{E}(N)\rangle_N$ (cf fourth row of Table II, and [5] for further details). Theory and numerics are compared in the bottom part of that figure.

### C. Triaxial case with rational frequencies

Now $Q_1$, $Q_2$ and $Q_3$ are positive integers and have pairwise irreducible ratios.

Since frequencies are integer, it produces families of classical periodic orbits (Lissajous figures). A perturbative treatment, similar to the isotropic case, can be done to obtain an explicit expression for the level density [11]. For convenience, the oscillating part of the level density is decomposed into two different parts (see Table II): $\widetilde{\rho}_I$ (resp. $\widetilde{\rho}_T$) which is connected to the level density of the isotropic (resp. triaxial with irrational frequency ratios) HO. Below, these two components are referred to as "isotropic" and "triaxial", respectively. We follow the same method as before in order to get expressions for $\widetilde{\mathcal{N}}(\mu)$ and $\widetilde{E}(N)$ (cf third column of Table II).

To understand in this case the $N$–dependence of the fluctuating part of the energy, it is useful to calculate the ratio

$$\mathcal{R}_T = \frac{\Lambda_T}{\Lambda_I} \tag{10}$$

of the typical amplitude of the triaxial component with respect to the isotropic one. These two amplitudes are approximated here by computing the amplitude of the first term $k = 1$ of the corresponding sum (cf Table II)

$$\Lambda_I = \frac{(3N)^{2/3}}{2\pi^2(Q_1Q_2Q_3)^{1/3}}\ , \tag{11}$$

$$\Lambda_T = \max\begin{pmatrix} Q_1/(4\pi^2|\sin(\pi Q_2/Q_1)\sin(\pi Q_3/Q_1)|) \\ Q_2/(4\pi^2|\sin(\pi Q_1/Q_2)\sin(\pi Q_3/Q_2)|) \\ Q_3/(4\pi^2|\sin(\pi Q_1/Q_3)\sin(\pi Q_2/Q_3)|) \end{pmatrix} \tag{12}$$

A finer estimate of $\Lambda_T$ requires an analysis of the number theoretic properties of the $k$-th dependence of the denominators in $\widetilde{E}_T$, that we shall not do here. Since, for given frequencies, $\Lambda_T$ is a constant independent of $N$, $\mathcal{R}_T \propto N^{-2/3}$. Thus, for any rational set of frequencies, there exists a critical number of particles $N_c$ above which the behavior of $\widetilde{E}(N)$ is dominated by the isotropic component. In this high–$N$ regime the behavior of $\widetilde{E}(N)$ qualitatively coincides, up to a rescaling of the overall amplitude by $(Q_1Q_2Q_3)^{-1/3}$ and of a rescaling of the phase by $(Q_1Q_2Q_3)^{1/3}$, with the behavior of the isotropic HO described in the subsection II.B. This corresponds to a regular (i.e. single–frequency) pattern of large amplitude oscillations (or shells), with clearly defined magic numbers, as a function of $N$ (compare Fig. 2 and the lower right panel of Fig. 3). The value of the magic numbers may be estimated similarly to the previous subsection. This behavior illustrates the occurrence of an increasing number of accidental degeneracies in the single–particle spectrum as $N$ increases (as already pointed out in Ref.[10] in the 2D case). This qualitative behavior is also valid for the axial symmetric case, where two integer frequencies are equal.

In contrast, in the limit $\mathcal{R}_T \gg 1$ ($N \ll N_c$), $\widetilde{E}(N)$ is controlled by the triaxial term of the shell energy, $\widetilde{E}_T$. As in the irrational case, the fluctuating part of the energy is now characterized by a roughly constant (and small, compared to the isotropic case) amplitude, with the gross features of the oscillations well approximated by the superposition of a small number of terms having different frequencies. In particular, for some triplet of frequencies, in the regime $N < N_c$ supershell-like structures may be observed, as illustrated for instance in Fig. 3.

In summary, in the triaxial rational case generically a transition at $\mathcal{R}_T \sim 1$ ($N \sim N_c$) from a triaxial regime ($\mathcal{R}_T \gg 1, N \ll N_c$) toward an isotropic behavior ($\mathcal{R}_T \ll 1, N \gg N_c$) is expected as $N$ increases. This behavior is illustrated for a particular set of frequencies in Fig. 3, where the transition $\mathcal{R}_T \sim 1$, estimated from Eqs.(10)–(12), occurs at $N_c \sim 131060$. The lower left and right panels of Fig. 3 focus on the two extreme limits.

Though we have not studied all the possible cases (axial symmetry, rational-irrational, etc), the above examples illustrate the variety of behaviors of energy fluctuations one can find as the frequency ratios are varied.

## III. SELF–BOUND SYSTEMS

Up to now we have considered non–interacting fermions in HO potentials that keep their shape (frequencies) fixed as the number of fermions is varied. Such a scheme is a good approximation for dilute Fermi gases in optical traps [7], or in quantum dots, where the external potential dominates over the mean–field interaction energy [7]. But self–bound systems, like metallic clusters or atomic nuclei, behave differently. In those systems the shape of the self–consistent mean field potential, determined from the minimization of the ground state energy with respect to deformations, may strongly depend on the number of particles $N$.

If the HO potential considered here is viewed as the self–consistent mean field potential, then at each $N$ the energy is minimized with respect to the three frequencies. Conservation of the volume implies that the product of the three frequencies remains constant [3], $Q_1Q_2Q_3 = cte$. The constant can be in fact a function of $N$, to mimic for instance the approximately constant nuclear density. But this acts as a multiplicative factor which can be absorbed into the frequencies. Hence, without loss of generality, we normalize this constant to one.

In the following we consider only axial symmetric deformations ($Q_1 = Q_2$). This simplification, though not exact, is known to provide a good approximation in most nuclear cases. We use the axially symmetric expression of the oscillating part of the energy computed analogously to the previous sections, with $Q_1$ and $Q_3$ two incommensurable real numbers with pairwise irrational ratio, and imposing the volume conservation. There is thus only one free parameter ($Q_1$), and we obtain

$$\begin{aligned}\widetilde{E}_{SB}(N) = & \frac{(3N)^{1/3}}{2\pi^2}\sum_{k=1}^{\infty}\frac{\sin(2\pi k(3N)^{1/3}/Q_1)}{k^2\sin(\pi k/Q_1^3)} \\ + & \frac{1}{4\pi^2Q_1^2}\sum_{k=1}^{\infty}\frac{\cos(\pi k/Q_1^3)\cos((2\pi k(3N)^{1/3}/Q_1))}{k^2\sin^2(\pi k/Q_1^3)} \\ + & \frac{1}{4\pi^2Q_1^2}\sum_{k=1}^{\infty}\frac{(-1)^{k+1}\cos((2\pi k(3N)^{1/3}Q_1^2))}{k^2\sin^2(\pi kQ_1^3)} \quad .(13)\end{aligned}$$

Using similar arguments as in previous sections, we keep only the first term in each sum of Eq.(13). Besides, as we must minimize the energy with respect to $Q_1$, the latter is a function of $N$. The term which comes from the first sum has the largest amplitude (this will be confirmed *a posteriori*, when the $N$–dependence of $Q_1$ will be know) [15]. So we can remove all other contributions from Eq.(13), keeping the simple approximation

$$\widetilde{E}_{SB}(N) = (3N)^{1/3}\frac{\sin(2\pi\ (3N)^{1/3}/Q_1)}{2\pi^2\sin(\pi/Q_1^3)}\ . \qquad (14)$$

For the minimization, we need also to evaluate $\bar{E}(N)$. The approximated (leading–order) TF chemical potential Eq.(8) used until now is not sufficiently accurate because it leads to a wrong TF ground state: the minimum of $\bar{E}$ doesn't give an isotropic shape. To obtain a better description of $\bar{E}$ we must improve the calculation of $\bar{\mu}_N$. This implies solving the full cubic equation given by the canonical condition $\bar{\mathcal{N}}(\bar{\mu}_N) = N$. We have done that using Cardano's formula [16], and obtained the result presented in the third row of Table I. Then, the analytic

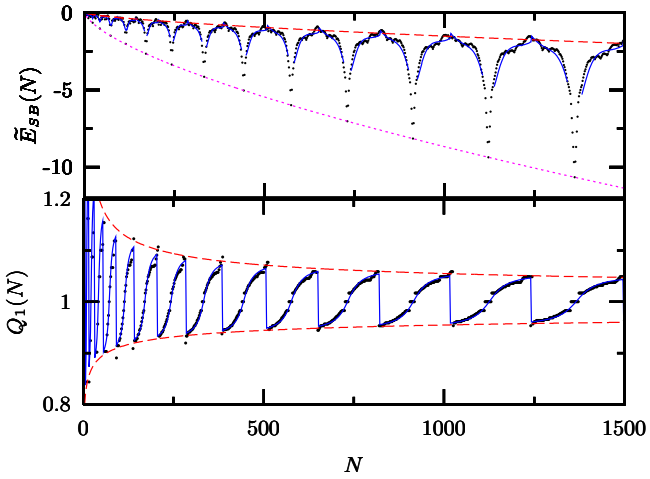


FIG. 4: (Color online) Upper panel: Oscillating part of the ground state energy as a function of $N$ computed numerically by the minimization of the energy of the free triaxial HO (dots). In full line we plot Eq. (14) using the phenomenological expression (21) for $\varepsilon$. In dashed line, analytic result for $\widetilde{E}_{SB}$ valid at mid–shells, Eq.(20). In dotted line, analytic result for $\widetilde{E}_{SB}$ for the magic numbers (Table II, case B, last row).
Lower panel: $Q_1 = (1+\varepsilon)^{-1/3}$ as a function of $N$ computed numerically by the minimization of the energy of the free triaxial HO (dots). In full line we plot $Q_1$ using the phenomenological expression (21) for $\varepsilon$. In dashed line, the mid–shell approximation, Eq.(19).

expression for the energy to be minimized is

$$E(N) = \frac{(3N)^{4/3}}{4} + \frac{(3N)^{2/3}}{24}\theta^{-2/3}(2+\theta^2) + \frac{\theta^{-4/3}}{2(12)^2}(2+\theta^2)^2 + \frac{(3N)^{1/3}\sin(2\pi(3N\theta)^{1/3})}{2\pi^2\sin(\pi\theta)} \ , \quad (15)$$

where

$$\theta = Q_3/Q_1 = Q_1^{-3} \ . \quad (16)$$

We assume now that the frequency ratio has the perturbative form $\theta = 1 + \varepsilon$ , where $|\varepsilon| \ll 1$ (small deformations). Since we know that close to magic numbers the system is spherical, we are interested in the behavior in–between shells. We thus concentrate our analysis of shell effects for values of $N$ close to the middle of the shells. From Eq.(15), we find that the middle of the shells correspond approximatively to values of $N$ given by $(3N)^{1/3} = (2i+1)/2$ , where $i \in \mathbb{N}$. Hence for these values of $N$, using a Taylor expansion of $\theta^{1/3}$ and the addition formula of the sine function, we get for the fluctuating part of the energy:

$$\widetilde{E}_{SB}(N) = \frac{(3N)^{1/3}}{2\pi^3\varepsilon}\sin\left(\frac{2\pi(3N)^{1/3}\varepsilon}{3}\right) \ . \quad (17)$$

The latter equation is the leading order in $\varepsilon$ of Eq.(15) (the smooth part is of lower order). The minimization of the energy is thus equivalent to the minimization of the function (17). We cancel the derivative of Eq.(17), to get

$$\frac{2\pi(3N)^{1/3}\varepsilon}{3} = \tan\left(\frac{2\pi(3N)^{1/3}\varepsilon}{3}\right) \ . \quad (18)$$

Note that $-\varepsilon$ is also a solution of Eq.(18) (prolate–oblate symmetry). In spite of the fact that Eq.(18) has many solutions, we keep of course the one that gives the smallest value of the function (17). We have solved numerically this equation for $\varepsilon$, and find that the solution is well approximated by

$$\varepsilon(N) = \pm 1.49 N^{-1/3} \ , \quad (19)$$

which gives, for the self–bound energy fluctuations at mid–shell

$$\widetilde{E}_{SB}(N) = -0.0152 N^{2/3} \ . \quad (20)$$

We have tested numerically these results (cf Fig. 4). They give a very good approximation of $\widetilde{E}_{SB}(N)$ in the mid–shell region, showing that the axially symmetric deformation is a good approximation. The weight of the fluctuating term at mid–shell is thus proportional to $N^{2/3}$, with a negative slope. This has the same $N$–dependence as the amplitude of the fluctuating part of an isotropic HO (whereas an axial–symmetric fixed potential yields instead a $N^{1/3}$ dependence), or to the subleading, surface term of the smooth part. This enhancement shows the fundamental importance of the $N$–dependence of the frequencies.

Beyond this simple approximation, we have also found a phenomenological expression of $\varepsilon$ which turns out to be a quite good approximation of the deformation for arbitrary $N$ (see bottom part of Fig. 4)

$$\varepsilon(N) = -\frac{\pi}{2(3N)^{1/3}}\arctan\left(2\pi((3N)^{1/3} - [(3N)^{1/3} + 1/2])\right), \quad (21)$$

where $[a]$ denotes here the integer part of $a$. This equation shows that the deformation is, up to a global damping factor $\propto N^{-1/3}$, a strictly periodic function of the variable $x = (3N)^{1/3}$, of period $\Delta x = 1$ (the same is valid for the shell correction energy). It gives an extremely accurate description of the $N$ dependence of the frequency, $Q_1 = [1+\varepsilon(N)]^{-1/3}$, see Fig. 4. Increasing the particle number $N$ from the value of a magic number (corresponding to $Q_1 = 1$), the frequency initially increases, $Q_1 > 1$, corresponding to a prolate shape (accordingly, $Q_3 < 1$). At mid-shell, the shape suddenly changes from prolate, $Q_1 > 1$, to oblate, $Q_1 < 1$, keeping its deviation from isotropy $|Q_1 - 1|$ constant. As $N$ further increases, $Q_1$ diminishes, to arrive finally at $Q_1 = 1$ again at the next magic number. The cycle starts again, with a decreasing overall amplitude.

Replacing Eq.(21) in Eq.(14) we obtain a rather good approximation of $\widetilde{E}_{SB}(N)$, see Fig. 4. Using the approx-

imation $\varepsilon \ll 1$, $\widetilde{E}_{SB}(N)$ can be written

$$\widetilde{E}_{SB}(N) = \frac{(3N)^{2/3}\sin\left(2\pi\ (3N)^{1/3}(1+\varepsilon(N))^{1/3}\right)}{\pi^4 \arctan\left(2\pi((3N)^{1/3}-[(3N)^{1/3}+1/2])\right)}, \tag{22}$$

where $\varepsilon(N)$ is given by Eq.(21). The results obtained with this equation are very similar to those of Eq.(14), shown in Fig. 4. This equation clearly shows the scaling $N^{2/3}$ of $\widetilde{E}_{SB}(N)$. Both the numerator and the denominator in Eq.(22) are functions of $N$ that oscillate around 0. The completely different behavior of $\widetilde{E}_{SB}(N)$ (a negative decreasing function, see Fig. 4) comes from a delicate balance between both oscillatory functions. Close to magic numbers, the amplitude of Eq.(22), not shown in the figure, is smaller than the numerical results; further corrections need to be included to improve in this region.

We can check that the amplitude $\Lambda_1$ of Eq.(22) (first term of the first sum in Eq.(13)) is dominant with respect to the amplitudes $\Lambda_2$ and $\Lambda_3$ of the first terms of the two remaining sums in Eq.(13), respectively. Using $Q_1^{-3} = \theta = 1+\varepsilon$, the value of $\varepsilon$ given by Eq.(19), and keeping only the first term of a Taylor expansion in $\varepsilon$ of the sine function in the denominators, one can easily check that $\Lambda_2/\Lambda_1 = \Lambda_3/\Lambda_1 \approx 0.07$. This justifies the approximation used.

Because the study of $E(N)$ for self–bound system is a minimization problem, we are not able to compute an explicit and general expression for the average of the fluctuating part of the energy, analogous to Eq.(6) but now valid for self–bound systems. Nevertheless, it follows from the previous results that the average scales as $N^{2/3}$. A numerical fit of the average of $\widetilde{E}_{SB}$, denoting

$$\langle \widetilde{E}_{SB}(N)\rangle_N = -a_{fit}N^{2/3}\ , \tag{23}$$

gives $a_{fit} = 0.0262$.

As an application of the previous results, we consider a schematic model of the atomic nucleus, with $N$ non–interacting neutrons and $N$ uncharged non–interacting protons whose mean–field potential is assumed to have an HO shape. In order to mimic the saturation properties of nuclear forces and get dimensional quantities we multiply $\widetilde{E}_{SB}$ by the factor $82A^{-1/3}$ MeV, where $A = 2N$ is the mass number [2]. The previous factor modifies the $N$ dependence of the amplitude of $\widetilde{E}_{SB}$, leading to an amplitude now proportional to $N^{1/3}$, instead of $N^{2/3}$. The energy is minimized as previously.

We compare the results of this model to one of the best theoretical models for the nuclear binding energy, based on an extension of the liquid drop model [8], see Fig. 5. The smooth part used in Ref. [8] being different from ours, it leads to a difference in the offset. In spite of that, we see that the qualitative properties of the simplified HO model, including the energy scale, are correct. In both cases we plot the numerical average of $\widetilde{E}_{SB}$. A negative slope of the fit in Ref. [8], consistent with $-a_{sw}N^{1/3}$, is observed, with a proportionality factor $a_{sw} = 1.93$ MeV. It is very similar from what we obtain from our simplified model ($a_{HO} = 1.71$ MeV, top part of Fig. 5). The shell amplitude as a function of $N$ is also well reproduced. Nevertheless no supershell structure occurs in our analysis [17], and magic numbers are badly estimated because we are not taking into account, in our simple model, spin-orbit effects [3].

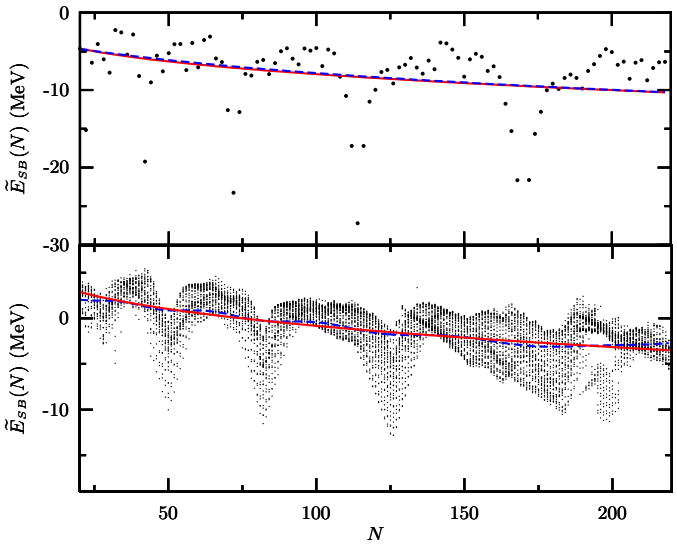


FIG. 5: (Color online) Upper panel: Numerical computation of $\widetilde{E}_{SB}$ as a function of the neutron number for the HO atomic nucleus model (dots). In dashed line, the numerical average of $\widetilde{E}_{SB}$ and in full line the phenomenological result adapted from Eq.(23): $\langle \widetilde{E}_{SB}(N)\rangle_N = -\ 1.71\ N^{1/3}$MeV
Lower panel: Ground state shell correction energy as a function of the neutron number from [8] (dots). In dashed line, the numerical average of $\widetilde{E}_{SB}$ and in full line the phenomenological fit: $\langle \widetilde{E}_{SB}(N)\rangle_N = (8.14 - 1.93N^{1/3})$ MeV.

## IV. CONCLUSION

For a Fermi gas treated in the mean–field approximation, we provided here a quantitative description of the ground–state shell correction energy. Two different possibilities were considered, fixed potentials and self–bound systems. We showed that very different qualitative behaviors may appear in harmonic traps, depending on the number–theoretic properties of the frequency ratios. Based on a semiclassical theory, we provided an analytic description of the different behaviors, as well as of the average of the shell energy. In spite of its simplicity, HO potentials show good qualitative agreement with more elaborate models. In self–bound systems, one of our main results is an accurate analytic description of

the deformation and of the shell correction energy as a function of the particle number.

A few periodic orbits were used to describe $\widetilde{E}(N)$. Although this is in general a good approximation, in some cases it fails. As discussed in [11] for $\widetilde{\rho}$, the triaxial irrational case with frequencies very close to each other can reproduce, to a good approximation, the isotropic case, but only if a large number of terms in the sums is included. Generically, the convergence properties of the sums over periodic orbits is a delicate problem, directly related to the number–theoretic properties of the frequency ratios. We haven't considered this problem in its full generality; it clearly deserves a closer inspection, in particular in connection with the minimization problem.

We have shown that, in self–bound systems, the properties of the shell correction energy scale as $-aN^{2/3}$ (or $-aN^{1/3}$, if saturation properties are taken into account), where $a$ is some positive constant. Although it compares favorably with realistic nuclear models, it should be noted that this behavior is specific of HO potentials. In fact, if one considers instead a hard–wall spherical potential, supershell structures will appear, and modulations of, e.g., the average of $\widetilde{E}_{SB}(N)$ are expected, as observed in metallic clusters [18]. These, however, are not observed experimentally in nuclear data, due to the limited number of nucleons (see, for instance, [17]). Deviations from an HO confining potential toward a more steeper one of the Woods–Saxon type are generically expected to be produced by interactions. Within a spherical symmetry, these deviations from an harmonic confinement were shown to lead to supershell effects [19]. We would like to thank Peter Schuck for usefull discussions.

This work was supported by grants ANR–05–Nano–008–02 and ANR–NT05–2–42103, by the IFRAF Institute.

[1] R. B. Wiringa, Steven C. Pieper Phys.Rev.Lett. 89 (2002) 182501; Steven C. Pieper, K. Varga, R. B. Wiringa, Phys. Rev. C **66** (2002) 044310; S. Bargi, G. M. Kavoulakis, S. M. Reimann, Phys. Rev. A 73 (2006) 033613.

[2] P. Ring and P. Schuck, *The Nuclear Many-Body Problem* (Springer-Verlag, Berlin, 1980).

[3] A. Bohr and B. R. Mottelson, *Nuclear Structure Vol.I* (Benjamin, Reading, Massachusetts, 1969).

[4] M. Brack and R. K. Bhaduri, *Semiclassical Physics* (Addison-Wesley, Reading, MA, 1997).

[5] M. Centelles, P. Leboeuf, A. Monastra, J. Roccia, P. Schuck and X. Viñas, Phys. Rev. C **74**, 034332 (2006).

[6] K. M. O'Hara *et al.*, Science **298**, 2179 (2002).

[7] R. Grimm, M. Weidemüller, Y. B. Ovchinnikov, Advances in Atomic, Molecular and Optical Physics **42**, 95 (2000); H. Heiselberg and B. Mottelson, Phys. Rev. Lett. **88**, 190401 (2002).

[8] P.M. Moller, J.R. Nix, W.D. Meyers, W.J. Swiatecki, At. Data Nucl. Data Tables **59**, 185 (1995).

[9] S. G. Nilsson, Kgl. Dan. Viden. Selsk. Mat. Fys. Medd. **29** No.16 (1955) 29

[10] A. Pandey, O. Bohigas, M. J. Giannoni, J. Phys. A **22**, 4083 (1989).

[11] M. Brack, S. Jain, Phys. Rev. A **51**, 3462 (1995).

[12] P. Meier, M. Brack, S. C. Creagh, Z. Phys. D **41**, 281 (1997).

[13] P. Leboeuf and A. G. Monastra, Ann. Phys. **297**, 127 (2002).

[14] H. Nishioka, K. Hansen, and B. R. Mottelson, Phys. Rev. B **42**, 9377 (1990).

[15] We may have chosen a rational frequency ratio between $Q_1$ and $Q_3$, instead of an irrational one. However, it can be shown that the isotropic term that appears for a rational ratio, discussed in section II.C, is not dominant at the middle of the shells, even in the limit $N \to \infty$, and that the analysis based on rational or irrational frequency ratios give similar results. This is due to the $N$–dependence of $Q_1$.

[16] M. Abramowitz and I. A. Stegun, *Handbook of Mathematical Functions with Formulas, Graphs, and Mathematical Tables, 9th printing* (New York: Dover, 1972).

[17] P. Leboeuf, *Regularity and chaos in the nuclear masses*, Lectures delivered at the VIII Hispalensis International Summer School, Sevilla, Spain, June 2003 (to appear in *Lecture Notes in Physics*, Springer–Verlag, Eds. J. M. Arias and M. Lozano); nucl-th/0406064.

[18] W. D. Knight, K. Clemenger, W. A. de Heer, W. A. Saunders, M. Y. Chou, and M. L. Cohen, Phys. Rev. Lett. **52**, 2141 (1984).

[19] Y.Yu, M. Ogren, S. Aberg, S. M. Reimann, M. Brack, Phys. Rev. A **72**, 051602(R) (2005).

| | |
|---|---|
| $\bar{\rho}(\epsilon)$ | $\frac{1}{Q_1Q_2Q_3}\left(\epsilon^2 - \frac{Q_1^2+Q_2^2+Q_3^2}{12}\right)$ |
| $\bar{\mathcal{N}}(\mu)$ | $\frac{1}{3Q_1Q_2Q_3}\left(\mu^3 - \frac{Q_1^2+Q_2^2+Q_3^2}{4}\mu\right)$ |
| $\bar{E}(N)$ | $\frac{1}{Q_1Q_2Q_3}\left(\frac{1}{4}(3Q_1Q_2Q_3N)^{4/3} + \frac{Q_1^2+Q_2^2+Q_3^2}{24}\,(3Q_1Q_2Q_3N)^{2/3} + \frac{(Q_1^2+Q_2^2+Q_3^2)^2}{2(12)^2} + \mathcal{O}(N^{-2/3})\right)$ |

TABLE I: The smooth part of the single–particle level density for a triplet of frequencies of the 3D harmonic potential as a function of the energy $\epsilon$ in the first row. Corresponding integrated level density up to an energy $\mu$ in the second row. Last row, the smooth part of the ground–state energy of the Fermi gas as a function of the number of particles $N$.

| | **A. Triaxial case with irrational frequencies** | **B. Isotropic case** | **C. Triaxial case with rational frequencies** |
|---|---|---|---|
| $\widetilde{\rho}(\epsilon)$ | $\frac{1}{Q_1}\sum_{k=1}^{\infty}\frac{(-1)^{k+1}\cos(2\pi k\epsilon/Q_1)}{\sin(\pi kQ_2/Q_1)\sin(\pi kQ_3/Q_1)}$ $+\frac{1}{Q_2}\sum_{k=1}^{\infty}\frac{(-1)^{k+1}\cos(2\pi k\epsilon/Q_2)}{\sin(\pi kQ_1/Q_2)\sin(\pi kQ_3/Q_2)}$ $+\frac{1}{Q_3}\sum_{k=1}^{\infty}\frac{(-1)^{k+1}\cos(2\pi k\epsilon/Q_3)}{\sin(\pi kQ_1/Q_3)\sin(\pi kQ_2/Q_3)}$ | $2\epsilon^2\sum_{k=1}^{\infty}(-1)^k\cos(2\pi k\epsilon)$ | $\widetilde{\rho}_I(\epsilon)+\widetilde{\rho}_T(\epsilon)$ $\widetilde{\rho}_I(\epsilon)=\frac{2\epsilon^2}{Q_1Q_2Q_3}\sum_{k=1}^{\infty}(-1)^{k(Q_1+Q_2+Q_3)}\cos(2\pi k\epsilon)$ $\widetilde{\rho}_T(\epsilon)=\frac{1}{Q_1}\sum_{k\neq lQ_1}^{\infty}\frac{(-1)^{k+1}\cos(2\pi k\epsilon/Q_1)}{\sin(\pi kQ_2/Q_1)\sin(\pi kQ_3/Q_1)}$ $+\frac{1}{Q_2}\sum_{k\neq lQ_2}^{\infty}\frac{(-1)^{k+1}\cos(2\pi k\epsilon/Q_2)}{\sin(\pi kQ_1/Q_2)\sin(\pi kQ_3/Q_2)}$ $+\frac{1}{Q_3}\sum_{k\neq lQ_3}^{\infty}\frac{(-1)^{k+1}\cos(2\pi k\epsilon/Q_3)}{\sin(\pi kQ_1/Q_3)\sin(\pi kQ_2/Q_3)}$ |
| $\widetilde{\mathcal{N}}(\mu)$ | $\frac{1}{2\pi}\sum_{k=1}^{\infty}\frac{(-1)^{k+1}\sin(2\pi k\mu/Q_1)}{k\sin(\pi kQ_2/Q_1)\sin(\pi kQ_3/Q_1)}$ $+\frac{1}{2\pi}\sum_{k=1}^{\infty}\frac{(-1)^{k+1}\sin(2\pi k\mu/Q_2)}{k\sin(\pi kQ_1/Q_2)\sin(\pi kQ_3/Q_2)}$ $+\frac{1}{2\pi}\sum_{k=1}^{\infty}\frac{(-1)^{k+1}\sin(2\pi k\mu/Q_2)}{k\sin(\pi kQ_1/Q_2)\sin(\pi kQ_3/Q_2)}$ | $\frac{\mu^2}{\pi}\sum_{k=1}^{\infty}(-1)^k\frac{\sin(2\pi k\mu)}{k}$ | $\widetilde{\mathcal{N}}_I(\mu)\ +\ \widetilde{\mathcal{N}}_T(\mu)$ $\widetilde{\mathcal{N}}_I(\mu)=\sum_{k=1}^{\infty}\frac{(-1)^{k(Q_1+Q_2+Q_3)}\mu^2\sin(2\pi k\mu)}{\pi kQ_1Q_2Q_3}$ $\widetilde{\mathcal{N}}_T(\mu)=\frac{1}{2\pi}\sum_{k\neq lQ_1}^{\infty}\frac{(-1)^{k+1}\sin(2\pi k\mu/Q_1)}{k\sin(\pi kQ_2/Q_1)\sin(\pi kQ_3/Q_1)}$ $+\frac{1}{2\pi}\sum_{k\neq lQ_2}^{\infty}\frac{(-1)^{k+1}\sin(2\pi k\mu/Q_2)}{k\sin(\pi kQ_1/Q_2)\sin(\pi kQ_3/Q_2)}$ $+\frac{1}{2\pi}\sum_{k\neq lQ_3}^{\infty}\frac{(-1)^{k+1}\sin(2\pi k\mu/Q_3)}{k\sin(\pi kQ_1/Q_3)\sin(\pi kQ_2/Q_3)}$ |
| $\widetilde{E}(N)$ | $\frac{Q_1}{4\pi^2}\sum_{k=1}^{\infty}\frac{(-1)^{k+1}\cos(2\pi k(3Q_2Q_3N/Q_1^2)^{1/3})}{k^2\sin(\pi kQ_2/Q_1)\sin(\pi kQ_3/Q_1)}$ $+\frac{Q_2}{4\pi^2}\sum_{k=1}^{\infty}\frac{(-1)^{k+1}\cos(2\pi k(3Q_1Q_3N/Q_2^2)^{1/3})}{k^2\sin(\pi kQ_1/Q_2)\sin(\pi kQ_3/Q_2)}$ $+\frac{Q_3}{4\pi^2}\sum_{k=1}^{\infty}\frac{(-1)^{k+1}\cos(2\pi k(3Q_1Q_2N/Q_3^2)^{1/3})}{k^2\sin(\pi kQ_1/Q_3)\sin(\pi kQ_2/Q_3)}$ | $\frac{(3N)^{2/3}}{2\pi^2}\sum_{k=1}^{\infty}\frac{(-1)^k}{k^2}\cos(2\pi k(3N)^{1/3})$ | $\widetilde{E}_I(N)+\widetilde{E}_T(N)$ $\widetilde{E}_I(N)=\sum_{k=1}^{\infty}\frac{(-1)^{k(Q_1+Q_2+Q_3)}(3N)^{2/3}\cos(2\pi k\ (3Q_1Q_2Q_3N)^{1/3})}{2\pi^2(Q_1Q_2Q_3)^{1/3}k^2}$ $\widetilde{E}_T(N)=\frac{Q_1}{4\pi^2}\sum_{k\neq lQ_1}^{\infty}\frac{(-1)^{k+1}\cos(2\pi k(3Q_2Q_3N/Q_1^2)^{1/3})}{k^2\sin(\pi kQ_2/Q_1)\sin(\pi kQ_3/Q_1)}$ $+\frac{Q_2}{4\pi^2}\sum_{k\neq lQ_2}^{\infty}\frac{(-1)^{k+1}\cos(2\pi k(3Q_1Q_3N/Q_2^2)^{1/3})}{k^2\sin(\pi kQ_1/Q_2)\sin(\pi kQ_3/Q_2)}$ $+\frac{Q_3}{4\pi^2}\sum_{k\neq lQ_3}^{\infty}\frac{(-1)^{k+1}\cos(2\pi k(3Q_1Q_2N/Q_3^2)^{1/3})}{k^2\sin(\pi kQ_1/Q_3)\sin(\pi kQ_2/Q_3)}$ |
| $\langle\widetilde{E}(N)\rangle_N$ | $\propto N^{-2/3}$ | $\frac{1}{24}(3N)^{2/3}$ | $\frac{(3N)^{2/3}}{24(Q_1Q_2Q_3)^{1/3}},\ \text{for}\ \mathcal{R}_T\ll 1$ $\propto N^{-2/3},\ \text{for}\ \mathcal{R}_T\gg 1$ |
| $\widetilde{E}_{MAGIC}(N)$ | | $-\frac{1}{24}(3N)^{2/3}$ | $\frac{-(3N)^{2/3}}{24(Q_1Q_2Q_3)^{1/3}},\ \text{for}\ \mathcal{R}_T\ll 1$ |

TABLE II: The three columns separate the different cases of the 3D harmonic potential studied in section II. The oscillating part of the single–particle level density for a triplet of frequencies as a function of the energy $\epsilon$ is given in the first row (from [11]). Corresponding integrated level density up to an energy $\mu$ in the second row. Third row, the oscillating part of the ground–state energy of the Fermi gas as a function of the number of particles $N$. The fourth row gives the analytic expression for the average of $\widetilde{E}$. In the last, when available, the analytic curve for the envelope of the magic numbers.